

# Using Human Ratings for Feedback Control: A Supervised Learning Approach with Application to Rehabilitation Robotics

Marcel Menner, Lukas Neuner, Lars Lünenburger, and Melanie N. Zeilinger

**Abstract**—This paper presents a method for tailoring a parametric controller based on human ratings. The method leverages supervised learning concepts in order to train a reward model from data. It is applied to a gait rehabilitation robot with the goal of teaching the robot how to walk patients physiologically. In this context, the reward model judges the physiology of the gait cycle (instead of therapists) using sensor measurements provided by the robot and the automatic feedback controller chooses the input settings of the robot so as to maximize the reward. The key advantage of the proposed method is that only a few input adaptations are necessary to achieve a physiological gait cycle. Experiments with non-disabled subjects show that the proposed method permits the incorporation of human expertise into a control law and to automatically walk patients physiologically.

**Index Terms**—Learning and Adaptive Systems, Human Feedback-based Control, Rehabilitation Robotics, Human-Centered Robotics.

## I. INTRODUCTION

Humans can perform very complex tasks that are difficult to achieve with autonomous systems. The dependency on human supervision or expertise still restricts efficient operation of many complex systems. An important domain where human expertise is usually needed is rehabilitation robotics, where we consider the robot-assisted gait trainer Lokomat® [1] in this paper, see Figure 1. Robotic systems like the Lokomat have recently been introduced in gait rehabilitation following neurological injuries with the goal of mitigating the limitations of conventional therapy [2]–[6]. However, training with such robots still requires the supervision and interaction of experienced therapists [1].

Gait rehabilitation with the Lokomat currently requires physiotherapists to manually adjust the mechanical setup and input settings, e.g. the speed of the treadmill or the range of motion, in order to bring patients into a physiological and safe gait cycle. Therapists have to be trained specifically for the device and acquire substantial experience in order to achieve good input settings. Although there are guidelines for their adjustments [7], it remains a heuristic process, which strongly depends on the knowledge and experience of the therapist. Automatic adaptation of input settings can reduce the duration of therapists’ schooling, improve patient training, make the technology more broadly applicable, and can be more cost effective. In this work, we propose a method to automatically adapt input settings. Although the motivation behind this work is in the domain of rehabilitation robotics, the proposed

M. Menner, L. Neuner, and M.N. Zeilinger are with the Institute for Dynamic Systems and Control, ETH Zurich, 8092 Zurich, Switzerland {mmenner, lneuner, mzeilinger}@ethz.ch

L. Lünenburger is with Hocoma AG, 8604 Volketswil, Switzerland lars.lünenburger@hocoma.com

method addresses general human-in-the-loop scenarios, where expert knowledge can improve system operation.

In this paper, we propose a two-step approach to achieve automatic input adaptations: First, we define a feature vector to characterize the gait cycle and postulate a reward model to judge the physiology of the gait cycle using the feature vector. The reward model is trained with therapists’ ratings using a supervised learning technique, where the feature vector is obtained from sensor measurements provided by the robot. The sensor measurements are the angle, torque, and power of both the hip and knee joints of the robot. Second, we use the gradient of the reward model to determine input adaptations that achieve the desired gait cycle. This involves a steady-state model to relate the gradient of the reward model with respect to the feature vector (high dimensional) to input settings (low dimensional) that adjust the gait cycle. A key component in the proposed formulation is that the reward model and its gradient are formulated as functions of the feature vector rather than the input settings. The high dimensionality of the feature vector allows us to use one model for all human subjects with very different body types, which enables very efficient online application of the proposed method. In order to train both the reward model and the steady-state model, we collected data with various physiological and non-physiological input settings from 16 non-disabled subjects. The subjects were instructed to be passive while being walked by the robot in order to imitate patients with limited or no ability to walk in the early stages of recovery. Experiments with ten non-disabled subjects highlighted the ability of the proposed method to improve the walking pattern within few adaptations starting from multiple initially non-physiological gait cycles.



Fig. 1. Lokomat® gait rehabilitation robot (Hocoma AG, Volketswil, CH).

## Related Work

Adaptive control strategies have been the subject of a body of research in robotic gait trainers with the goal of improving the therapeutic outcome of treadmill training [8]–[13]. The work in [8] presents multiple strategies for automatic gait cycle adaptation in robot-aided gait rehabilitation based on minimizing the interaction torques between device and patient. Biomechanical recordings to provide feedback about a patient’s activity level are introduced in [9], [10]. Automated synchronization between treadmill and orthosis based on iterative learning is introduced in [11]. In [12], a path control method is introduced to allow voluntary movements along a physiological path defined by a virtual tunnel. An algorithm to adjust the mechanical impedance of an orthosis joint based on the level of support required by a patient is proposed in [13]. Further research in the domain of rehabilitation robotics is presented, e.g., in [14], [15]. In [14], the human motor system is modeled and analyzed as approximating an optimization problem trading off effort and kinematic error. In [15], a patient’s psychological state is estimated to judge their mental engagement.

Related fields are gait cycle classification [16]–[19], reinforcement learning from human feedback [20]–[27], or inverse learning methods [28]–[41]. Differing from gait cycle classification methods [16]–[19], this paper does not aim to identify a human’s individual gait but to generalize the classification of a physiological gait using data from multiple humans. Further, we infer the physiology of the gait from data and use the gathered knowledge for feedback control. Reinforcement learning uses a trial and error search to find a control policy [42]. The framework proposed in [20] allows human trainers to shape a policy using approval or disapproval. In [21], human-generated rewards within a reinforcement learning framework are employed to control a 2-joint velocity control task. In [22], human feedback is not used as a reward signal but utilized as a direct policy label. In [23], human preferences are learned through ratings based on a pairwise comparison of trajectories. In [24], a robot motion planning problem is considered, where users provide a ranking of paths that enable the evaluation of the importance of different constraints. In [25], a method is presented that actively synthesizes queries to a user to update a distribution over reward parameters. In [26], user preferences in a traffic scenario are learned based on human guidance in terms of feature queries. In [27], human ratings are used to learn a probabilistic Markov model. However, the online application of these methods typically requires a few hundred human ratings to learn a policy. This is infeasible when working with a patient, where a comparatively small number of feedback rounds has to be sufficient. In inverse reinforcement learning [28]–[34] and inverse optimal control [35]–[41], demonstrations from humans are utilized to learn a reward/objective function instead of ratings.

## II. HARDWARE DESCRIPTION & PROBLEM DEFINITION

The Lokomat® gait rehabilitation robot (Hocoma AG, Volketswil, CH) is a bilaterally driven gait orthosis that is attached to the patient’s legs by Velcro straps. In conjunction

with a bodyweight support system, it provides controlled flexion and extension movements of the hip and knee joints in the sagittal plane. Leg motions are repeated based on predefined but adjustable reference trajectories. Additional passive foot lifters ensure ankle dorsiflexion during swing. The bodyweight support system partially relieves patients from their bodyweight via an attached harness. A user interface enables gait cycle adjustments by therapists via a number of input settings [1], [10].

*Input Settings:* One important task of the therapist operating the Lokomat is the adjustment of the input settings to obtain a desirable gait trajectory. A total of 13 input settings can be adjusted to affect the walking behavior, which are introduced in Table I. In this work, we propose a method that can automate or assist the therapists in the adjustment of the input settings by measuring the gait cycle.

TABLE I  
INPUT SETTINGS OF THE LOKOMAT

| Input Setting & Description                                | Step-size  | Range          |
|--|------------|----------------|
| Hip Range of Motion (Left & Right)                         | 3°         | 23°, 59°       |
| Defines the amount of flexion and extension                |            |                |
| Hip Offset (Left & Right)                                  | 1°         | -5°, 10°       |
| Shifts movements towards extension or flexion              |            |                |
| Knee Range of Motion (Left & Right)                        | 3°         | 32°, 77°       |
| Defines amount of flexion                                  |            |                |
| Knee Offset (Left & Right)                                 | 1°         | 0°, 8°         |
| Shifts movement into flexion for hyperextension correction |            |                |
| Speed  | 0.1km/h    | 0.5km/h, 3km/h |
| Sets the treadmill speed                                   |            |                |
| Orthosis speed   | 0.01       | 0.15, 0.8      |
| Defines the orthosis and affects walking cadence           |            |                |
| Bodyweight Support   | continuous | 0kg, 85kg      |
| Defines carried weight for unloading                       |            |                |
| Guidance Force   | 5%         | 0%, 100%       |
| Sets amount of assistance                                  |            |                |
| Pelvic   | 1cm        | 0cm, 4cm       |
| Defines lateral movement                                   |            |                |

### A. State-of-the-Art Therapy Session

The current practice of gait rehabilitation with the Lokomat includes the preparation and setup of the patient and device, actual gait training, and finally removing the patient from the system [7]. Gait training is further divided into three phases:

1. Safe walk: The patient is gradually lowered until the dynamic range for bodyweight support is reached. The purpose of this first phase is to ensure a safe and non-harmful gait cycle.
2. Physiological walk: After ensuring safe movements, the gait cycle is adjusted so that the patient is walked physiologically by the robot.
3. Goal-oriented walk: The gait cycle is adjusted to achieve therapy goals for individual sessions while ensuring that the patient’s gait remains physiological.

In this paper, we focus on the physiological walk. In a state-of-the-art therapy session, therapists are advised to follow published heuristic guidelines on how to adjust the input settings based on observations in order to reach a physiological walk. Three examples of the heuristic guidelines are as follows: If

the step length does not match walking speed, then the hip range of motion or treadmill speed should be adjusted; if the initial contact is too late, then hip offset or the hip range of motion should be decreased; if the foot is slipping, then the synchronization should be increased or the knee range of motion decreased. An extended overview of heuristics can be found in [7]. This heuristic approach requires experience and training with experts, which incurs high costs and limits the availability of the rehabilitation robot due to the small number of experienced experts. The proposed method aims to alleviate this limitation as described in the following.

### B. Technological Contribution

We propose a method for automatically suggesting suitable input settings for the Lokomat based on available sensor measurements in order to walk patients physiologically. The proposed framework can be used for recommending input settings for therapists, automatic adaptation of input settings, or as an assistive method for therapists during schooling with the Lokomat. Figure 2 illustrates the proposed method as a recommendation system. The method is derived assuming that the mechanical setup of the Lokomat is done properly, such that the purpose of adapting the input settings is the improvement of the gait cycle and not corrections due to an incorrect setup.

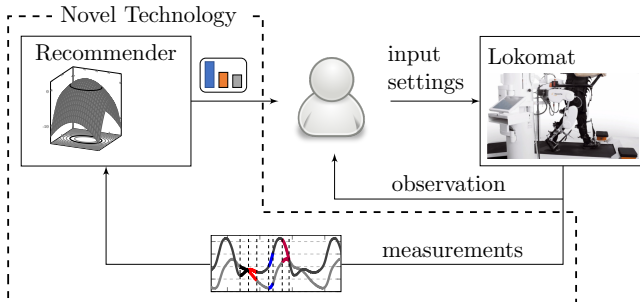


Fig. 2. Overview of the proposed method as a recommendation system. The novel technology (dashed lines) augments the state-of-the-art control loop of a therapist and the Lokomat. Sensor measurements of angle, torque, and power of both hip and knee joints provided by the Lokomat are used to compute recommendations for the input adaptations.

### III. CONTROLLER DESIGN BASED ON HUMAN RATINGS

This section describes the proposed human feedback-based controller. In the setup considered, input settings  $s \in \mathbb{R}^m$  of the controlled system lead to a gait cycle represented by a feature vector  $x \in \mathbb{R}^n$  in steady-state:

$$x = f(s), \quad (1)$$

where  $f$  is an unknown function. For the application considered, the input settings  $s$  are given in Table I and the feature vector  $x$  is composed of the statistical features of measurements, which characterize the gait cycle and are further discussed in Section IV. Here, the notion of a steady-state means that any transients due to an input adaptation have faded. The control objective is to find input settings  $s^*$  for which  $x^* = f(s^*)$  represents a desired system state, i.e. a physiological gait cycle in the considered application.

**Control Law and Conceptual Idea:** The method is based on a reward model, reflecting the control objective, and a steady-state model, associating a feature vector with an input setting. The reward model is a function that assigns a scalar value to the feature vector estimating an expert rating of the 'goodness' of the feature vector. The reward thereby provides a direction of improvement for the feature vector, which is mapped to a change in input settings via the steady-state model.

We define the control law in terms of input adaptations  $\Delta s$ :

$$\Delta s = f^{-1}(\alpha \Delta x + x) - s,$$

where  $\Delta x$  is the direction of improvement,  $f^{-1} : \mathbb{R}^n \rightarrow \mathbb{R}^m$  is the steady-state model (the inverse mapping of  $f(\cdot)$  in (1)), and  $\alpha > 0$  is the gain of the control law. We compute  $\Delta x$  as the gradient of the reward model  $r(x) \in \mathbb{R}$ , i.e.

$$\Delta x = \nabla_x r(x).$$

Figure 3 shows an example of a reward model and indicates how its gradient is used for feedback control using the steady-state model. Both models  $r(x)$  and  $f^{-1}(\cdot)$  are inferred from data. In order to train the reward model, we utilize ratings on an integer scale as samples of the reward model, i.e.  $r_i = 1, \dots, S$ , where  $r_i = 1$  is the worst and  $r_i = S$  is the best rating. Additionally, we train a steady-state model  $f^{-1}(\cdot)$  to relate the direction of improvement suggested by the reward model to the corresponding input adaptation (bottom part of Figure 3). In order to build both the reward model and the steady-state model,  $N$  training samples are collected. Each training sample

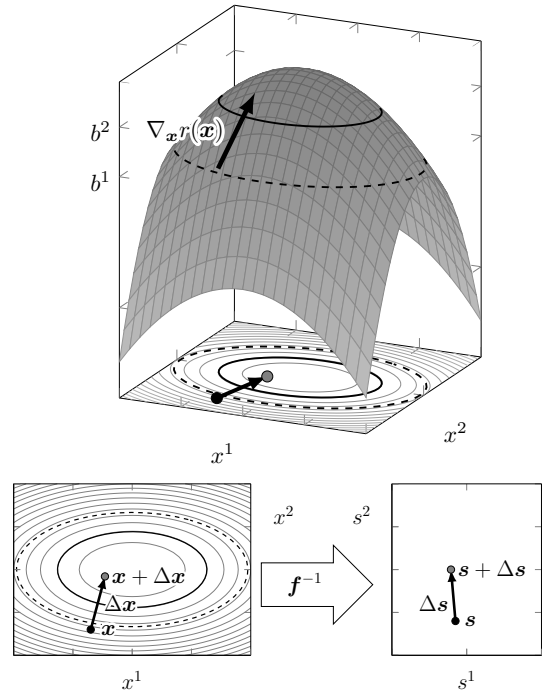


Fig. 3. Top: Example of reward model with gradient vector  $\nabla_x r(x)$  where  $x = [x^1 x^2]^T$  and projected level sets onto the  $x^1 - x^2$  plane. The example shows a case of three ratings  $r_i = 1, 2, 3$  separated by two classification boundaries indicated as solid black and dashed black ellipses. Bottom: steady-state model to compute  $\Delta s$  from  $\Delta x$  where  $s = [s^1 s^2]^T$ .

with index  $i$  consists of a feature vector  $\mathbf{x}_i$ , the input settings  $\mathbf{s}_i$ , and the corresponding rating  $r_i \in \{1, \dots, S\}$ :

$$\{\mathbf{x}_i, \mathbf{s}_i, r_i\}_{i=1}^N. \quad (2)$$

Note that throughout this paper, the feature vector  $\mathbf{x}$  is normalized using collected data  $\mathbf{x}_i$  such that the collected data are zero-mean with unit-variance in order to account for different value ranges and units, cf. [43].

*Outline:* The reward model is trained with the feature vector  $\mathbf{x}_i$  and its corresponding rating  $r_i$  in (2) using a supervised learning technique (Section III-A). The resulting reward model is then used to compute the gradient  $\nabla_{\mathbf{x}} r(\mathbf{x})$  as direction of improvement. Finally, a steady-state model relates this direction of improvement with necessary changes in input settings  $\mathbf{s}$ . The steady-state model is computed using a regression technique (Section III-B).

### A. Reward Model using Supervised Learning

The first step of the framework is the learning of a reward model reflecting the physiology of the gait based on supervised learning techniques [43]. The reward model is a continuous function, i.e. it provides a reward for all  $\mathbf{x}$ , whereas observations  $\mathbf{x}_i$  are potentially sparse.

In view of the considered application, we postulate a reward model of the form:

$$r(\mathbf{x}) = 0.5\mathbf{x}^T \mathbf{W} \mathbf{x} + \mathbf{w}^T \mathbf{x} + b, \quad (3)$$

where  $\mathbf{W} = \mathbf{W}^T \prec 0$ ,  $\mathbf{w} \in \mathbb{R}^n$ , and  $b \in \mathbb{R}$  are the parameters to be learned from expert ratings given in the form of integers on a scale from 1 to  $S$ . The rationale for selecting a quadratic model with negative definite  $\mathbf{W}$  is the observation that gait degrades in all relative directions when changing input settings. Important properties of this reward model are that a vanishing gradient indicates that global optimality has been reached and its computational simplicity. This motivates the gradient ascent method for optimizing performance.

In order to learn  $\mathbf{W}$ ,  $\mathbf{w}$ , and  $b$  in (3), we construct  $S - 1$  classification problems of the form one-vs.-all [43]. These  $S - 1$  classification problems share the parameters  $\mathbf{W}$ ,  $\mathbf{w}$ , and  $b$  of the reward model and the corresponding classification boundaries are given by

$$r^l(\mathbf{x}) = 0.5\mathbf{x}^T \mathbf{W} \mathbf{x} + \mathbf{w}^T \mathbf{x} + b^l$$

for all  $l = 1, \dots, S - 1$  with  $b^l = b - l - 0.5$  separating the  $S$  different ratings such that  $r^l(\mathbf{x}_i) > 0$  if  $r_i > l + 0.5$ . Further, for each data sample  $i$  and each  $l$ , we define

$$y_i^l = \begin{cases} 1 & \text{if } r_i > l + 0.5 \\ -1 & \text{else.} \end{cases}$$

Hence, an ideal reward model with perfect data and separation satisfies

$$y_i^l r^l(\mathbf{x}_i) \geq 0 \quad \forall i = 1, \dots, N \quad \forall l = 1, \dots, S - 1. \quad (4)$$

In order to allow for noisy data and imperfect human feedback, (4) is relaxed to find  $r^l(\mathbf{x})$  that satisfies (4) 'as closely as possible' by introducing a margin  $\xi_i^l \geq 0$ . This approach is

closely related to a Support Vector Machine, cf. [43], with a polynomial kernel function of degree two. The functions  $r^l(\mathbf{x})$  correspond to  $S - 1$  classification boundaries in a multi-category classification framework. The parameters  $\mathbf{W}$ ,  $\mathbf{w}$ , and  $b$  of the reward model (3) are computed by solving the following optimization problem:

$$\begin{aligned} \text{minimize}_{\mathbf{W}, b^l, \mathbf{w}, \xi_i^l} \quad & \sum_{l=1}^{S-1} \sum_{i=1}^N \xi_i^l + \lambda_1 \cdot \|\mathbf{W}\|_1 + \lambda_2 \cdot \|\mathbf{w}\|_1 \\ \text{subject to} \quad & y_i^l (r^l(\mathbf{x}_i)) \geq 1 - \xi_i^l \quad \forall i = 1, \dots, N \\ & \xi_i^l \geq 0 \quad \forall l = 1, \dots, S - 1 \\ & r^l(\mathbf{x}_i) = 0.5\mathbf{x}_i^T \mathbf{W} \mathbf{x}_i + \mathbf{w}^T \mathbf{x}_i + b^l \\ & b^l = b - l - 0.5 \\ & \mathbf{W} = \mathbf{W}^T \prec 0 \end{aligned} \quad (5)$$

where  $\lambda_1, \lambda_2 > 0$  control the trade-off between minimizing the training error and model complexity captured by the norm  $\|\mathbf{W}\|_1 = \sum_{j=1}^n \sum_{k=1}^n |W_{jk}|$  (elementwise 1-norm) and  $\|\mathbf{w}\|_1$ , which is generally applied to avoid overfitting of a model and is sometimes also called lasso regularization [43].

### B. Feedback Control using Reward Model

The second step of the proposed framework is to exploit the trained reward model for feedback control. The idea is (i) to use the gradient of the reward model as the direction of improvement and (ii) to relate this gradient to a desired change in inputs with a steady-state model.

(i) *Gradient of reward model:* The gradient of the inferred reward model is the direction of best improvement. The control strategy is to follow this gradient in order to maximize reward. The gradient of the proposed quadratic reward model is

$$\Delta \mathbf{x} = \nabla_{\mathbf{x}} r(\mathbf{x}) = \mathbf{W} \mathbf{x} + \mathbf{w}.$$

(ii) *Mapping of gradient to setting space with steady-state model:* In order to advance the system along the gradient direction, we relate the direction of improvement  $\Delta \mathbf{x}$  to a change in input settings with a steady-state model  $\mathbf{f}^{-1}(\cdot)$ . We use a linear model  $\mathbf{s} \approx \mathbf{M} \mathbf{x}$  with  $\mathbf{M} \in \mathbb{R}^{m \times n}$  to compute the change in input settings  $\Delta \mathbf{s}$  as

$$\Delta \mathbf{s} = \mathbf{M}(\alpha(\mathbf{W} \mathbf{x} + \mathbf{w}) + \mathbf{x}) - \mathbf{s}, \quad (6)$$

where  $\alpha$  can be interpreted as feedback gain or the learning rate in a gradient ascent method.  $\mathbf{M}$  can be interpreted as a first order approximation of  $\mathbf{f}^{-1}(\cdot)$  and is estimated as the least squares solution of all data samples in (2):

$$\text{minimize}_{\mathbf{M}} \quad \sum_{i=1}^N \|\mathbf{s}_i - \mathbf{M} \mathbf{x}_i\|_2^2 + \lambda_3 \cdot \|\mathbf{M}\|_1 \quad (7)$$

where, again, we use  $\lambda_3 > 0$  to control the trade-off between model fit and model complexity.

**Remark 1.** As we will show in the analysis in Section V, the linear mapping  $\mathbf{s} \approx \mathbf{M} \mathbf{x}$  yields sufficient accuracy for the application considered. For more complex systems, one might consider a different steady-state model, e.g. higher order polynomials or a neural network to approximate  $\mathbf{f}^{-1}(\cdot)$ .

Using the quadratic reward model in (3) and the linear steady-state model in (7), the application of the proposed control strategy (6) requires only matrix-vector multiplications, which is computationally inexpensive and can be performed online, cf. Algorithm 1 for an overview of the method. Additionally, as will be shown empirically, the application requires only few online input adaptations.

#### Algorithm 1 Training and Application of the Method

|   |                    |
|---|--------------------|
| <b>Training</b>   | ▷ rating needed    |
| 1: Collect data set in (2).   |                    |
| 2: Compute reward model $\mathbf{W}$ , $\mathbf{w}$ , and $\mathbf{b}$ with (5) and steady-state model $\mathbf{M}$ with (7). |                    |
| <b>Online Algorithm</b>   | ▷ no rating needed |
| 3: <b>do</b>  |                    |
| 4: Obtain feature vector $\mathbf{x}$ from measurement.   |                    |
| 5: Apply input adaptation $\Delta \mathbf{s} = \mathbf{M}(\alpha(\mathbf{Wx} + \mathbf{w}) + \mathbf{x}) - \mathbf{s}$ .      |                    |
| 6: Wait until steady state is reached.  |                    |
| 7: <b>while</b> stopping criterion not fulfilled  | ▷ cf. Section IV-D |

**Remark 2.** *In principle, Bayesian optimization or reinforcement learning could be applied to directly learn physiological settings. The proposed two-step and model-based method, in contrast, makes use of the higher dimensionality of the feature vector to characterize the gait cycle. This approach has the key advantage that less samples are required online and thus, less steps to find physiological settings, which is essential for the application considered.*

**Remark 3.** *It is similarly possible to determine the direction of improvement using second order derivatives of the reward model, e.g. using a Newton-Raphson method. We choose the gradient as the best (local) improvement.*

**Remark 4.** *The proposed method iteratively approaches the optimal settings  $\mathbf{s}^*$  with the gradient ascent method. This is important for the considered application to cautiously adapt the input settings of the robot with a human in the loop.*

## IV. ADAPTATION OF GAIT REHABILITATION ROBOT TO WALK PATIENTS PHYSIOLOGICALLY

In this section, we show how to apply the method presented in Section III to automatically adjust, or recommend a suitable adjustment, of the Lokomat's input settings in order to walk patients physiologically. A core element is the reward model that has been built on therapists' ratings and is used to judge the physiology of the gait. For simplicity, we adjust settings for the left and right leg symmetrically. This does not pose a problem for the presented study with non-disabled subjects but might be revisited for impaired subjects in future work.

In this work, we focus on physiological walk and exclude the guidance force and the pelvic input settings as they are mainly used for goal-oriented walk [7]. This exclusion is valid for physiological walk where the guidance force and pelvic settings are kept constant at 100% and 0cm, respectively. Hence, there are seven input settings that are considered in the application of the method. The proposed method is implemented to augment a previously developed safety controller

that ensures safe operation of the Lokomat. In this way, the overall behavior is guaranteed to have the necessary safety requirements for patient and robot, yet among the safe input settings, the ones that improve the gait cycle are chosen.

### A. Gait Cycle

The walking of a human is a repetitive sequence of lower limb motions to achieve forward progression. The gait cycle describes such a sequence for one limb and commonly defines the interval between two consecutive events that describe the heel strike (initial ground contact) [44]. The gait cycle is commonly divided into two main phases, the stance and the swing phase. The stance phase refers to the period of ground contact, while the swing phase describes limb advancement. Figure 4 illustrates the subdivision of these two main phases of the gait cycle into multiple sub-phases, beginning and ending with the heel strike. This results in a common description of gait using a series of discrete events and corresponding gait phases [44]. We focus on four particular phases of the gait cycle, which are emphasized in Figure 4:

- Heel strike: The moment of initial contact of the heel with the ground.
- Mid-stance: The phase in which the grounded leg supports the full body weight.
- Toe off: The phase in which the toe lifts off the ground.
- Mid-swing: The phase in which the raised leg passes the grounded leg.

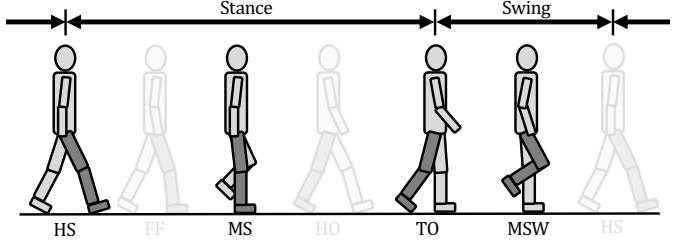


Fig. 4. Gait phases in order: Heel strike (HS), foot flat (FF), mid-stance (MS), heel off (HO), toe off (TO), mid-swing (MSW). Both FF and HO phase are not rated in this work, but presented for consistency with the literature [44].

### B. Evaluation of Gait Cycle and Data Collection

The four phases are used to derive the reward model. For evaluating the four gait phases, we introduce a scoring criterion in consultation with experienced therapists:

Rating 1: Safe, but not physiological.

Rating 2: Safe, not entirely physiological gait cycle.

Rating 3: Safe and physiological gait cycle.

*Data Collection:* A total of 16 non-disabled subjects participated in the data collection. The 16 subjects were between 158cm - 193cm (5'2" - 6'4") in height, 52kg - 93kg (115lbs - 205lbs) in weight, and aged 25 - 62. Informed consent for the use of the data has been received from all human subjects. Each experiment involved an evaluation of the four gait phases by therapists for several input settings to collect data in a wide

range of gait cycles. The non-disabled subjects were instructed to be passive throughout data collection, i.e. they were walked by the robot. This allowed us to collect data for both physiological and non-physiological gait cycles. Measurements of the Lokomat were recorded for all evaluations. At the beginning of each experiment, the experienced therapists manually tuned the input settings to achieve rating 3 for all four phases. Note that the input settings resulting in a physiological walking pattern varied between subjects. The selected input settings are given in the Appendix.

The scoring criterion and the consideration of the four phases, as well as the experiment protocol were introduced in consultation with clinical experts from Hocoma (U. Costa and P. A. Gonçalves Rodrigues, personal communication, Nov. 05, 2017). As a result, we obtained the chosen input settings, the corresponding ratings on an integer scale from 1 to 3, and the recording of measurements of the Lokomat. Next, we discuss the computation of the feature vector from the recorded measurements.

**Feature Vector:** We use the gait index signal of the Lokomat as an indicator to identify progression through the gait cycle. The gait index is a sawtooth signal and is displayed in the bottom plot in Figure 5. It is used to determine the time-windows of the four phases, cf. the dashed lines in Figure 5. The time-windows are used to compute the feature vector, composed of statistical features for power, angle, and torque for both hip and knee joints, cf. Table II. The result is one feature vector for each phase:  $\mathbf{x}_{\text{HS}}, \mathbf{x}_{\text{MS}}, \mathbf{x}_{\text{TO}}, \mathbf{x}_{\text{MSW}} \in \mathbb{R}^{12}$ . The Lokomat provides measurements of all the signals listed in Table II synchronized by the gait index signal, which makes the computation of the features simple.

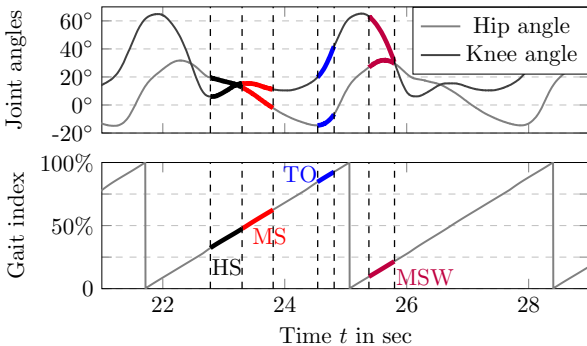


Fig. 5. Top: Joint angles. Bottom: Segmentation of time signals into four phases using the gait index with HS in 34.5%-47.5%, MS in 47.5%-65.5%, TO in 84.5%-92.5%, and MSW in 9.5%-21.5% of one period of the gait index. The falling edge of the gait index does not align with the biomechanical definition of a gait cycle but enables separation of the gait cycle into phases.

**Remark 5.** For each subject, the data collection as described in the Appendix takes around one hour, including rating the gait cycle. As described in Algorithm 1, the application of the control law does not include further training and the control law is therefore not personalized to the subject.

**Remark 6.** Initially, we defined more features than the twelve in Table II, e.g. frequency domain features, which the supervised learning problem in (5) with L1 regularization

TABLE II  
VALUES FOR FEATURE VECTOR

| #        | Joint | Signal      | Unit | Feature  |
|----------|-------|-------------|------|----------|
| $x^1$    | hip   | joint power | Nm/s | mean     |
| $x^2$    | hip   | angle       | rad  | min      |
| $x^3$    | hip   | angle       | rad  | max      |
| $x^4$    | hip   | angle       | rad  | range    |
| $x^5$    | hip   | torque      | Nm   | mean     |
| $x^6$    | hip   | torque      | Nm   | variance |
| $x^7$    | knee  | joint power | Nm/s | mean     |
| $x^8$    | knee  | angle       | rad  | min      |
| $x^9$    | knee  | angle       | rad  | max      |
| $x^{10}$ | knee  | angle       | rad  | range    |
| $x^{11}$ | knee  | torque      | Nm   | mean     |
| $x^{12}$ | knee  | torque      | Nm   | variance |

discarded. In order to reduce the problem dimension in the online algorithm, we discarded them as well.

### C. Reward Model and Steady-State Model for Lokomat

Given the data set, we apply the method in Section III to learn four reward models. We obtain a reward model for each of the four phases represented as  $\mathbf{W}_j, \mathbf{w}_j$ , and  $b_j$  from solving (5), where  $j \in \{\text{HS, MS, TO, MSW}\}$ .

The steady-state model  $\mathbf{M} \in \mathbb{R}^{7 \times 48}$  in (7) is computed by stacking the features of the four phases:

$$\mathbf{x} = [\mathbf{x}_{\text{HS}}^T \quad \mathbf{x}_{\text{MS}}^T \quad \mathbf{x}_{\text{TO}}^T \quad \mathbf{x}_{\text{MSW}}^T]^T.$$

### D. Control Law for Gait Rehabilitation Robot

Once the four reward models and the steady-state model are trained using the data in (2), the control law automatically proposes modifications to the input settings given the current measurements, i.e. it does not require ratings from therapists. The input adaptation  $\Delta s$  is computed as

$$\Delta s = \mathbf{M} \left( \begin{bmatrix} \alpha(\mathbf{W}_{\text{HS}} \mathbf{x}_{\text{HS}} + \mathbf{w}_{\text{HS}}) + \mathbf{x}_{\text{HS}} \\ \alpha(\mathbf{W}_{\text{MS}} \mathbf{x}_{\text{MS}} + \mathbf{w}_{\text{MS}}) + \mathbf{x}_{\text{MS}} \\ \alpha(\mathbf{W}_{\text{TO}} \mathbf{x}_{\text{TO}} + \mathbf{w}_{\text{TO}}) + \mathbf{x}_{\text{TO}} \\ \alpha(\mathbf{W}_{\text{MSW}} \mathbf{x}_{\text{MSW}} + \mathbf{w}_{\text{MSW}}) + \mathbf{x}_{\text{MSW}} \end{bmatrix} \right) - s.$$

While  $\Delta s$  yields continuous values, the input settings are adjusted in discrete steps, cf. the step-sizes in Table I. We aim to change one setting at a time, which is common practice for therapists [7] and eases the evaluation. The following suggests a method to select one single adaptation from  $\Delta s$ .

**Input Setting Selection & Stopping Criterion:** In order to select one single discrete change in input setting, we normalize  $\Delta s$  to account for different value ranges and different units per individual setting and select the input corresponding to the largest in absolute value:

$$k^* = \arg \max_{k=1, \dots, 7} \left| \frac{\Delta s^k}{\bar{s}^k - \underline{s}^k} \right|$$

with associated index  $k^*$ , where the normalization  $\bar{s}^k - \underline{s}^k$  is the range of the input setting  $k$  in Table I. Hence, the algorithm chooses one adaptation with step-size in Table I. The input adaptation is stopped when the largest normalized absolute value of change is smaller than a pre-defined parameter  $\beta$ , i.e.  $|\Delta s^{k^*}| / (\bar{s}^{k^*} - \underline{s}^{k^*}) \leq \beta$ . This indicates closeness to the optimum, i.e. that a physiological gait is reached.

## V. MODEL EVALUATION IN SIMULATION

We first analyze the algorithm in simulation to investigate the model quality. In this simulation study, we compare two reward models: One that uses ratings on an integer scale from 1 to 3 ( $S = 3$  in (5)) and one that uses only binary ratings, i.e. good and bad ( $S = 2$  in (5)). For the case  $S = 3$ , we use the collected ratings without modification. For the case  $S = 2$ , we combine the data points with rating 1 and rating 2 as *bad samples of gait* with  $r_i = 1$  and use the data points with rating 3 as *good samples of gait* with  $r_i = 2$ .

### A. Evaluation Metrics and Results

In order to evaluate the trained models, we split the experimentally collected data into training (80%) and validation data (20%). This split is done randomly and repeated 500 times to assess the robustness of the models. This technique is known as 5-fold cross validation [45] and ensures that the validation data is not biased by training on the same data.

1) *Evaluation of Reward Model:* We evaluate the accuracy of the reward model by computing the classification error as the pairwise difference in estimated rewards  $r(\mathbf{x}_i) - r(\mathbf{x}_j)$  for two data samples  $i$  and  $j$ , classified with respect to their ratings  $r_i$  and  $r_j$ . This is a suitable metric as two different ratings should be distinguishable. We define  $\Delta\bar{r}_{nm}$  as

$$\Delta\bar{r}_{nm} = \frac{1}{|I_n||I_m|} \sum_{i \in I_n} \sum_{j \in I_m} (r(\mathbf{x}_i) - r(\mathbf{x}_j)), \quad (8)$$

where  $I_n = \{i | r_i = n\}$  is an index set of data points with ratings  $r_i = n$ . If the trained reward model and data were perfect,  $\Delta\bar{r}_{nm} = n - m$  with zero standard deviation.

Table III reports the mean and standard deviation of  $\Delta\bar{r}_{nm}$  in (8) over the 500 splits of training and validation data. For the reward model computed with  $S = 3$ , the overall deltas in estimated rewards match the deltas in ratings very closely with 2.00 for  $\Delta\bar{r}_{31}$ , 0.97 for  $\Delta\bar{r}_{32}$ , and 1.03 for  $\Delta\bar{r}_{21}$ . For the reward model computed with  $S = 2$ , the overall deltas in estimated rewards match the delta in ratings very closely for  $\Delta\bar{r}_{32}$ . The estimated rewards for  $\Delta\bar{r}_{31}$  and  $\Delta\bar{r}_{21}$  are less accurate with 1.51 and 0.51, respectively.

TABLE III  
MEAN AND STANDARD DEVIATION OF CLASSIFICATION ERROR

| Three ratings (1, 2, or 3) $S = 3$   |                      |                      |                      |
|--------------------------------------|----------------------|----------------------|----------------------|
| Gait Phase                           | $\Delta\bar{r}_{31}$ | $\Delta\bar{r}_{32}$ | $\Delta\bar{r}_{21}$ |
| Heel Strike                          | 1.86 $\pm$ 0.052     | 0.92 $\pm$ 0.049     | 0.94 $\pm$ 0.055     |
| Mid-Stance                           | 2.04 $\pm$ 0.074     | 1.01 $\pm$ 0.048     | 1.02 $\pm$ 0.085     |
| Toe Off                              | 2.12 $\pm$ 0.046     | 1.03 $\pm$ 0.056     | 1.08 $\pm$ 0.069     |
| Mid-Swing                            | 1.96 $\pm$ 0.044     | 0.88 $\pm$ 0.058     | 1.08 $\pm$ 0.062     |
| Overall                              | 2.00 $\pm$ 0.033     | 0.97 $\pm$ 0.031     | 1.03 $\pm$ 0.042     |
| Binary ratings (good or bad) $S = 2$ |                      |                      |                      |
| Gait Phase                           | $\Delta\bar{r}_{31}$ | $\Delta\bar{r}_{32}$ | $\Delta\bar{r}_{21}$ |
| Heel Strike                          | 1.18 $\pm$ 0.054     | 0.80 $\pm$ 0.058     | 0.38 $\pm$ 0.047     |
| Mid-Stance                           | 1.78 $\pm$ 0.054     | 1.23 $\pm$ 0.061     | 0.55 $\pm$ 0.057     |
| Toe Off                              | 1.62 $\pm$ 0.048     | 0.96 $\pm$ 0.063     | 0.66 $\pm$ 0.053     |
| Mid-Swing                            | 1.47 $\pm$ 0.050     | 0.97 $\pm$ 0.053     | 0.50 $\pm$ 0.041     |
| Overall                              | 1.51 $\pm$ 0.033     | 1.01 $\pm$ 0.037     | 0.51 $\pm$ 0.027     |

2) *Evaluation of Steady-State Model:* The steady-state model is evaluated using the prediction error  $\bar{e}^k$  defined as

$$\bar{e}^k = \frac{1}{N} \sum_{i=1}^N |s_i^k - \mathbf{M}_{k*} \mathbf{x}_i|, \quad (9)$$

where  $k$  is the index of the input setting and  $\mathbf{M}_{k*}$  is the  $k$ th row of matrix  $\mathbf{M}$ . As we use normalized values for the input settings with  $s_i^k \in [0, 1]$ , the error  $\bar{e}^k$  can be interpreted as a percentage value in the range of the input settings.

Table IV reports mean and standard deviation of the errors  $\bar{e}^k$  in (9) over the 500 random splits of training and validation data for all input settings  $k$ . It shows an overall average error of less than 5% and that the errors for all input settings are consistently lower than 6%.

TABLE IV  
MEAN AND STANDARD DEVIATION OF STEADY-STATE MODEL

| $s^k$   | Setting              | Error $\bar{e}^k$   |
|---------|----------------------|---------------------|
| $s^1$   | Hip Range of Motion  | 0.0578 $\pm$ 0.0019 |
| $s^2$   | Hip Offset           | 0.0370 $\pm$ 0.0008 |
| $s^3$   | Knee Range of Motion | 0.0547 $\pm$ 0.0021 |
| $s^4$   | Knee Offset          | 0.0324 $\pm$ 0.0009 |
| $s^5$   | Speed                | 0.0307 $\pm$ 0.0009 |
| $s^6$   | Orthosis Speed       | 0.0315 $\pm$ 0.0010 |
| $s^7$   | Body Weight Support  | 0.0542 $\pm$ 0.0017 |
| Overall |                      | 0.0417 $\pm$ 0.0186 |

3) *Evaluation of Overall Algorithm:* We evaluate the performance of the overall algorithm by comparing the collected data with the output of the algorithm. Let the changes in input settings during data collection for all data samples  $i = 1, \dots, N$  be  $\Delta s_i^{\text{ex}} = s^{\text{ex}} - s_i$ , where  $s_i$  are the input settings of data point  $i$  and  $s^{\text{ex}}$  are the physiological settings, which are set by the therapist at the beginning of the experiment. Note that  $s^{\text{ex}}$  depends on the subject, however, we omit this dependency in the notation for ease of exposition. It is also important to note that  $s^{\text{ex}}$  are not the only possible physiological input settings. We compare the input adaptation proposed by our algorithm  $\Delta s_i$  against the deviation from the physiological settings  $\Delta s_i^{\text{ex}}$ , where we can have three different outcomes:

*Case 1 (Same Setting & Same Direction):* The algorithm selects the input adaptation in the same direction as during data collection, which is known to be a correct choice as it is closer to the physiological settings  $s^{\text{ex}}$ .

*Case 2 (Same Setting & Opposite Direction):* The algorithm selects the same setting but in the opposite direction as during data collection, which is likely to be an incorrect choice.

*Case 3 (Different Setting):* The algorithm selects a different input adaptation, the implications of which are unknown and could be either correct or incorrect, which cannot be evaluated without closed-loop testing.

We compute the percentage of data points falling in each case for each setting  $k$  and for  $\Delta s_i^{\text{ex}} = 0$  (no adaptation), i.e.  $p_{C1}^k, p_{C2}^k$ , and  $p_{C3}^k$  for Case 1, Case 2, and Case 3, respectively, where  $p_{C1}^k + p_{C2}^k + p_{C3}^k = 1$ . If the algorithm replicated the data collection perfectly, then  $p_{C1}^k = 1$  for all settings  $k$ . Given the discrete and unique setting selection, the overall algorithm has 15 options to choose from: An increase in one of the seven

settings by one unit, a decrease in one of the seven settings by one unit, or *no adaptation*. Hence, random decision-making yields a probability of  $p = 1/15 \approx 6.7\%$  for each option.

Table V reports mean and standard deviation of the percentage values of the three cases. The algorithm chooses the input adaptations for hip range of motion, hip offset, knee range of motion, and knee offset very often when their adaptation leads to  $s^{\text{ex}}$  (86.7% to 100.0%). Also, it often chooses *no adaptation* when the gait is physiological, with input settings  $s^{\text{ex}}$ . Table V also shows that decision-making with the proposed algorithm is more ambiguous for the input adaptations of speed, orthosis speed, and bodyweight support. Overall, the algorithm proposes a setting that is closer to  $s^{\text{ex}}$  (Case 1) in 80.7% and 80.6% for the reward models trained with  $S = 3$  and  $S = 2$ , respectively. The algorithm suggests a probably incorrect input adaptation in less than 1% (Case 2). In around 19%, the algorithm suggests a different input adaptation (Case 3).

TABLE V  
EVALUATION OF OVERALL ALGORITHM IN SIMULATION

| $s^k$ | Setting              | Three ratings (1, 2, or 3) $S = 3$   |                 |                 |
|-------|----------------------|--------------------------------------|-----------------|-----------------|
|       |                      | $p_{C1}^k$ in %                      | $p_{C2}^k$ in % | $p_{C3}^k$ in % |
|       | No Adaptation        | 77.6 $\pm$ 3.6                       | -               | 22.4 $\pm$ 3.6  |
| $s^1$ | Hip Range of Motion  | 86.7 $\pm$ 1.8                       | 0               | 13.3 $\pm$ 1.8  |
| $s^2$ | Hip Offset           | 96.4 $\pm$ 1.0                       | 0               | 3.6 $\pm$ 1.0   |
| $s^3$ | Knee Range of Motion | 91.0 $\pm$ 1.7                       | 0               | 9.1 $\pm$ 1.7   |
| $s^4$ | Knee Offset          | 100.0 $\pm$ 0.0                      | 0               | 0               |
| $s^5$ | Speed                | 71.1 $\pm$ 2.8                       | 0               | 29.0 $\pm$ 2.8  |
| $s^6$ | Orthosis Speed       | 33.3 $\pm$ 3.7                       | 3.5 $\pm$ 1.6   | 63.2 $\pm$ 3.8  |
| $s^7$ | Body Weight Support  | 55.6 $\pm$ 3.8                       | 0               | 44.5 $\pm$ 3.8  |
|       | Overall accuracy     | 80.7 $\pm$ 1.0                       | 0.3 $\pm$ 0.1   | 19.0 $\pm$ 1.0  |
| $s^k$ | Setting              | Binary ratings (good or bad) $S = 2$ |                 |                 |
|       |                      | $p_{C1}^k$ in %                      | $p_{C2}^k$ in % | $p_{C3}^k$ in % |
|       | No Adaptation        | 76.8 $\pm$ 3.7                       | -               | 23.2 $\pm$ 3.7  |
| $s^1$ | Hip Range of Motion  | 88.6 $\pm$ 1.7                       | 0               | 11.4 $\pm$ 1.7  |
| $s^2$ | Hip Offset           | 95.6 $\pm$ 1.1                       | 0               | 4.4 $\pm$ 1.1   |
| $s^3$ | Knee Range of Motion | 90.0 $\pm$ 2.0                       | 0               | 10.0 $\pm$ 2.0  |
| $s^4$ | Knee Offset          | 100.0 $\pm$ 0.0                      | 0               | 0               |
| $s^5$ | Speed                | 71.3 $\pm$ 2.9                       | 0               | 28.7 $\pm$ 2.9  |
| $s^6$ | Orthosis Speed       | 32.1 $\pm$ 3.8                       | 2.9 $\pm$ 1.4   | 65.0 $\pm$ 3.9  |
| $s^7$ | Body Weight Support  | 53.9 $\pm$ 3.9                       | 0               | 46.2 $\pm$ 3.9  |
|       | Overall accuracy     | 80.6 $\pm$ 1.1                       | 0.2 $\pm$ 0.1   | 19.2 $\pm$ 1.0  |

## B. Discussion

The reward model trained with binary ratings is very precise for ratings 3 and 2. This is sensible since the algorithm separates the samples with rating 3 from both ratings 2 and 1 by introducing one classification boundary at 2.5. This reward model also estimates that the data points with rating 1 are worse than rating 2 ( $\Delta\bar{r}_{21} = 0.51$ ). This is desirable but non-trivial as the data points with ratings 1 and 2 are not explicitly separated in the training. The rewards predicted with the reward model trained with three ratings (two classification boundaries at 1.5 and 2.5), match very closely for all ratings.

The steady-state model shows an average error of 5%. As we will show in Section VI, this accuracy suffices for the application considered. For example, the expected error of 3.07% of  $s^5$  translates into an error in treadmill speed of

0.075m/s and the expected error of 5.78% of  $s^1$  translates into an error in hip range of motion of 2.08°, which is less than one input setting step-size, cf. Table I. Even though another model may increase accuracy, it may come at the expense of increased complexity in the computation. Our linear model only requires matrix-vector multiplication, which can easily be implemented on the controller of the Lokomat and is chosen as a suitable compromise of simplicity and accuracy.

The evaluation of both components, the reward model and the steady-state model, in simulation allow us to conclude that they provide suitable models for the application considered. For the overall algorithm, Case 1 is known to result in an improved physiology of the gait cycle. Case 3, however, does not imply that the suggested adaptation will not lead to an improved gait cycle as there may be multiple different input adaptations that lead to a physiological gait (not only  $s^{\text{ex}}$ ). In these cases, we do not know if the suggested adaptation would have led to an improvement in gait without closed-loop testing. Hence, the probabilities 80.7% and 80.6% of Case 1 for the two reward models can be interpreted as a lower bound for the overall improvement. The relatively low standard deviation for all settings indicates that the learning is robust against variation in the training data. The use of binary ratings eases the data collection and has been shown to perform similarly well. Therefore, we proceed with closed-loop testing of the algorithm using a reward model trained with binary ratings.

## VI. EXPERIMENTAL RESULTS - CLOSED-LOOP TESTING

The proposed algorithm was implemented as a recommendation system on the Lokomat for closed-loop evaluation. We implemented the algorithm using the reward model trained with binary ratings (good and bad) of the gait cycle. It is important to note, that no data from the respective test person was used for training of the reward model or the steady-state model. We conducted 63 experimental trials with ten human subjects and various sets of initially non-physiological gait cycles. The guidance force was set to 100% for all trials. The treadmill speed was varied between 1.4km/h and 2.3km/h. Two therapists assessed the input adaptations suggested by the algorithm and rated whether the gait was physiological. The therapists implemented the input adaptations until the algorithm indicated that a physiological gait cycle had been reached. Additionally, the therapists indicated when they thought that a physiological gait had been reached and the algorithm should be stopped.

Table VI describes the ten different test scenarios that were used and outlines input adaptations that therapists are expected to make (according to the heuristic guidelines). Scenario 1 through 8 are very common observations of a patient's gait cycle. Scenario 9 and 10 are combinations of different observations and are included to challenge the algorithm with more complex scenarios. Ten non-disabled subjects participated in the closed-loop tests, where each subject underwent at least five experimental trials. The difference in the number of experimental trials is due to each subject's availability. However, the test scenarios were chosen so that each scenario was tested comparably often. Similarly to the data collection, the subjects were instructed to be as passive as possible.

TABLE VI  
TEST SCENARIOS OF EXPERIMENT

| Scenario: Observations                           | Therapists' heuristic rules (expectation)   |
|--|---|
| 1: Limited foot clearance, foot dropping         | Increase knee range of motion ( $s^3 \uparrow$ )  |
| 2: Short steps                                   | Increase hip range of motion, speed ( $s^1 \uparrow, s^5 \uparrow$ )  |
| 3: Foot dragging                                 | Decrease speed, increase orthosis speed ( $s^5 \downarrow, s^6 \uparrow$ )  |
| 4: Large steps, late heel strike                 | Decrease hip range of motion, hip offset ( $s^1 \downarrow, s^2 \downarrow$ )   |
| 5: Short steps, hip extension                    | Increase hip range of motion, hip offset ( $s^1 \uparrow, s^2 \uparrow$ )   |
| 6: Bouncing                                      | Decrease speed, body weight support ( $s^5 \downarrow, s^7 \downarrow$ )  |
| 7: Foot slipping                                 | Decrease knee range of motion, orthosis speed ( $s^3 \downarrow, s^6 \downarrow$ )  |
| 8: Knee buckling                                 | Increase knee range of motion, bodyweight support ( $s^3 \uparrow, s^7 \uparrow$ )  |
| 9: Large steps, early heel strike                | Decrease hip range of motion, increase hip offset, increase speed ( $s^1 \downarrow, s^2 \uparrow, s^5 \uparrow$ )                                  |
| 10: Large steps, late heel strike, foot slipping | Decrease hip range of motion, hip offset, knee range of motion, orthosis speed ( $s^1 \downarrow, s^2 \downarrow, s^3 \downarrow, s^6 \downarrow$ ) |

### A. Results

Figure 6 illustrates eight representative trials with the first subject. It contains four types of information and is separated by therapist in columns and by test scenario in rows:

- The sum of the ratings for the four phases ( $y$ -axis) over the number of applied changes ( $x$ -axis);
- the applied input adaptations and their direction, e.g.  $s_1 \uparrow$  represents an increase of Setting 1 by one unit;
- a statement from the therapists about the algorithm's suggested input adaptation, i.e. agreement with the suggestion as check mark  $\checkmark$ , disagreement as cross  $\times$ , and uncertainty about the suggestion as question mark  $?$ ; and
- the reaching of a physiological gait judged by the therapist with square markers (for the usage as recommendation system) and by the algorithm with diamond markers (for the usage as automatic adaptation system).

In all eight illustrated experiments, the algorithm provides a reliable, although not monotonic, improvement in the physiology of the gait. The input adaptations suggested by the algorithm led to a physiological gait for both the usage as recommendation system (square marker) and automatic adaptation system (diamond marker) in less than 10 adaptations with an overall rating of greater than or equal to 11, where 12 is the maximum possible rating. The input adaptations during the test of Scenario 1 with both therapists (first row) are similar to the heuristic guidelines in Table VI, i.e. an increase in the knee range of motion ( $s^3 \uparrow$ ). The input adaptations for Scenario 2 (second row) are different from the heuristic guidelines. Here, the algorithm converges to a kinematically different but physiological gait that is achieved through a slower treadmill speed and input settings that are adjusted accordingly. For Scenario 9 and 10 (third and fourth row), the algorithm achieved a physiological gait through adaptations that are similar to the heuristic guidelines. In all illustrated cases, the algorithm converges to a physiological gait.

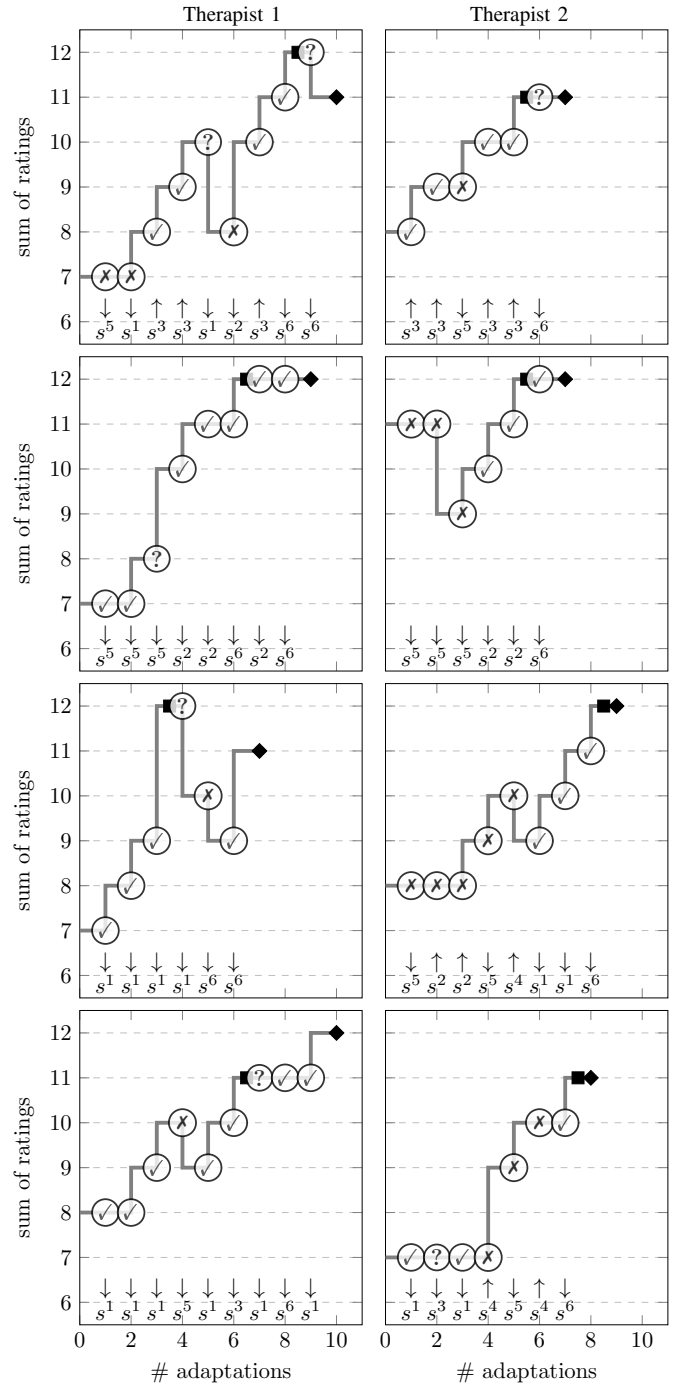


Fig. 6. Experimental evaluation of the closed-loop recommendation system for Scenarios 1, 2, 9, and 10 in Table VI (from top to bottom). Averaged for the eight experiments, a physiological gait was reached after 6.0 input adaptations (until square marker).

Table VII summarizes all 63 experimental trials with ten subjects. On average, after a proposed input adaptation, the gait cycle improved in 63% and did not degrade in 93% of adaptations. The latter percentage is important as sometimes, changing an input setting by only one unit is too small to make a noticeable change in the gait cycle and a couple of consecutive adaptations are necessary, e.g. for the orthosis speed ( $s^6$ ). Overall, the average number of adaptations per trial (APT) to reach a physiological gait cycle is 6.0.

TABLE VII  
SUMMARY OF ALL EXPERIMENTAL TRIALS

| Subject (body type)    | Trials | APT | Physiology of gait |              |
|------------------------|--------|-----|--------------------|--------------|
|                        |        |     | improved           | not degraded |
| 1 (193cm,93kg,male)    | 8      | 6.0 | 65%                | 92%          |
| 2 (195cm,100kg,male)   | 5      | 3.8 | 89%                | 100%         |
| 3 (163cm,53kg,female)  | 6      | 6.8 | 68%                | 98%          |
| 4 (175cm,85kg,female)  | 5      | 4.8 | 58%                | 92%          |
| 5 (172cm,68kg,female)  | 9      | 4.9 | 57%                | 89%          |
| 6 (190cm,85kg,male)    | 5      | 7.4 | 54%                | 97%          |
| 7 (167cm,85kg,male)    | 6      | 7.2 | 60%                | 93%          |
| 8 (180cm,75kg,male)    | 5      | 7.0 | 60%                | 83%          |
| 9 (167cm,64kg,female)  | 7      | 5.7 | 65%                | 97%          |
| 10 (161cm,48kg,female) | 7      | 6.9 | 71%                | 92%          |
| Overall                | 63     | 6.0 | 63%                | 93%          |

## B. Discussion

In general, the algorithm reaches a physiological gait cycle within very few adaptations. This observation supports our motivation for using this two-step algorithm. The majority of times, the therapists agreed with the suggestions from the algorithm, i.e. the suggested adaptations were conform with the heuristic tuning guidelines and their experience. Consequently, the resulting gait cycle was mostly kinematically similar to the one that the therapists would have chosen. In some notable instances, the therapists disagreed or were uncertain about the proposition and were surprised by the improvement in the gait cycle, e.g. Row 1, Therapist 1, Adaption 6; Row 2, Therapist 1, Adaption 3; or Row 4, Therapist 2, Adaption 4 in Figure 6. These instances are examples of situations where the algorithm chooses input adaptations, which were unknown to the therapists. In these cases, the resulting gait cycle was sometimes kinematically different to the heuristic guidelines, e.g. a gait with slower treadmill speed. Table VII shows that the algorithm is able to cope with various body types with similar results for all individuals.

It is worth noting that the differences between similar scenarios with two different therapists in Figure 6 and the same initial input settings do not necessarily lead to the same adjustments of input settings. This observation can be explained as the physiology of the gait does not only depend on the chosen input settings but also on the hardware setup, e.g. tightness of straps, which differs slightly between therapists. However, even though the hardware was setup slightly differently by the two therapists, the algorithm managed to find input settings that walk the subject physiologically, suggesting that the algorithm is robust to slight variations in the hardware.

## VII. CONCLUSION AND FUTURE WORK

This paper has derived a supervised learning-based method utilizing human ratings for learning parameters of a feedback controller. The approach was applied to the Lokomat robotic gait trainer with the goal of automatically adjusting the input settings to reach a physiological gait cycle by encapsulating the therapists' expertise in a reward model. Feedback control was enabled by this reward model and a steady-state model, which allows for converting desired changes in gait into input

adaptations. Experiments with human subjects showed that the therapists' expertise in the form of ratings of four gait phases provides sufficient information to discriminate between physiological and non-physiological gait cycles. Furthermore, the provided adaptations led to an improvement of the gait cycle towards a physiological one within fewer than ten adaptations. The physiological gait cycle was partly reached by changes in input settings that domain experts would not have chosen themselves, suggesting that the proposed method is capable of generalizing from ratings and proposing improved settings for unseen scenarios.

Future work involves the data collection, evaluation, and validation of the proposed method with impaired patients. This will include the assessment of asymmetric gait adaptations for the right and left legs, which can readily be achieved by considering one feature vector for each leg. Further, physical limitations and/or constraints in the patients' movements could be assessed online using sensor measurements of the Lokomat and considered for the selection of input settings.

## APPENDIX: EXPERIMENT SETUP

Each subject walked for approximately 60 seconds for each input setting, while the therapist provided evaluations of the walking pattern. The assessment started after a transient interval of approximately 15 seconds to ensure that the walking has reached a steady state. Table VIII shows the input settings as deviation of an initial physiological gait (IPG).

TABLE VIII  
INPUT SETTING FOR DATA COLLECTION

| Set | Input Settings      | Value                                  |
|-----|---------------------|--|
| 1   | Initial Set         | IPG                                    |
| 2   |                     | IPG + 0.5 $\frac{\text{km}}{\text{h}}$ |
| 3   | Speed               | IPG + 1.0 $\frac{\text{km}}{\text{h}}$ |
| 4   |                     | IPG - 0.5 $\frac{\text{km}}{\text{h}}$ |
| 5   |                     | IPG - 1.0 $\frac{\text{km}}{\text{h}}$ |
| 6   |                     | IPG + 0.03                             |
| 7   | Orthosis Speed      | IPG + 0.05                             |
| 8   |                     | IPG - 0.03                             |
| 9   |                     | IPG - 0.05                             |
| 10  |                     | IPG + 15%                              |
| 11  | Body Weight Support | IPG + 30%                              |
| 12  |                     | IPG - 15%                              |
| 13  |                     | IPG - 30%                              |
| 14  |                     | IPG + 6°                               |
| 15  | Hip ROM             | IPG + 12°                              |
| 16  |                     | IPG - 6°                               |
| 17  |                     | IPG - 12°                              |
| 18  |                     | IPG + 12°, IPG - 3°                    |
| 19  | Hip ROM, Offset     | IPG + 12°, IPG + 3°                    |
| 20  |                     | IPG - 12°, IPG - 3°                    |
| 21  |                     | IPG - 12°, IPG + 3°                    |
| 22  |                     | IPG + 4°                               |
| 23  | Hip Offset          | IPG + 8°                               |
| 24  |                     | IPG - 5°                               |
| 25  |                     | IPG + 6°                               |
| 26  | Knee ROM            | IPG + 12°                              |
| 27  |                     | IPG - 9°                               |
| 28  |                     | IPG - 15°                              |
| 29  | Knee ROM, Offset    | IPG + 15°, IPG + 6°                    |
| 30  |                     | IPG + 21°, IPG + 6°                    |
| 31  | Knee Offset         | IPG + 4°                               |
| 32  |                     | IPG + 8°                               |

## ACKNOWLEDGMENT

We gratefully acknowledge Patricia Andreia Gonçalves Rodrigues, Ursula Costa, and Serena Maggioni for their clinical support and invaluable discussions; Luca Somaini and Nils Reinert for their technical support; and Liliana Pavel for implementing the user interface.

## REFERENCES

- [1] G. Colombo, M. Joerg, R. Schreier, V. Dietz *et al.*, “Treadmill training of paraplegic patients using a robotic orthosis,” *J. Rehab. Res. and Develop.*, vol. 37, no. 6, pp. 693–700, 2000.
- [2] D. J. Reinkensmeyer, J. L. Emken, and S. C. Cramer, “Robotics, motor learning, and neurologic recovery,” *Annu. Rev. Biomed. Eng.*, vol. 6, pp. 497–525, 2004.
- [3] J. L. Emken and D. J. Reinkensmeyer, “Robot-enhanced motor learning: accelerating internal model formation during locomotion by transient dynamic amplification,” *IEEE Trans. Neural Syst. Rehab. Eng.*, vol. 13, no. 1, pp. 33–39, 2005.
- [4] L. Marchal-Crespo and D. J. Reinkensmeyer, “Review of control strategies for robotic movement training after neurologic injury,” *Journal of neuroengineering and rehabilitation*, vol. 6, no. 1, p. 20, 2009.
- [5] O. Lambery, L. Lünenburger, R. Gassert, and M. Bolliger, “Robots for measurement/clinical assessment,” in *Neurorehabilitation technology*. Springer, 2012, pp. 443–456.
- [6] H. M. Van der Loos, D. J. Reinkensmeyer, and E. Guglielmelli, “Rehabilitation and health care robotics,” in *Springer handbook of robotics*. Springer, 2016, pp. 1685–1728.
- [7] Hocoma, “Instructor script Lokomat training,” Hocoma AG, Tech. Rep., 2015.
- [8] S. Jezernik, G. Colombo, and M. Morari, “Automatic gait-pattern adaptation algorithms for rehabilitation with a 4-dof robotic orthosis,” *IEEE J. Robot. Automat.*, vol. 20, no. 3, pp. 574–582, 2004.
- [9] R. Riener, L. Lünenburger, S. Jezernik, M. Anderschitz, G. Colombo, and V. Dietz, “Patient-cooperative strategies for robot-aided treadmill training: First experimental results,” *IEEE Trans. Neural Syst. Rehab. Eng.*, vol. 13, no. 3, pp. 380–394, 2005.
- [10] R. Riener, L. Lünenburger, and G. Colombo, “Human-centered robotics applied to gait training and assessment,” *J. Rehab. Res. and Develop.*, vol. 43, no. 5, pp. 679–694, 2006.
- [11] A. Duschau-Wicke, J. Von Zitzewitz, R. Banz, and R. Riener, “Iterative learning synchronization of robotic rehabilitation tasks,” *Proc. IEEE Int. Conf. Rehab. Robotics*, pp. 335–340, 2007.
- [12] A. Duschau-Wicke, J. von Zitzewitz, A. Caprez, L. Lünenburger, and R. Riener, “Path control: a method for patient-cooperative robot-aided gait rehabilitation,” *IEEE Trans. Neural Syst. Rehab. Eng.*, vol. 18, no. 1, pp. 38–48, 2010.
- [13] S. Maggioni, L. Lünenburger, R. Riener, and A. Melendez-Calderon, “Robot-aided assessment of walking function based on an adaptive algorithm,” *Proc. IEEE Int. Conf. Rehab. Robotics*, pp. 804–809, 2015.
- [14] J. L. Emken, R. Benitez, A. Sideris, J. E. Bobrow, and D. J. Reinkensmeyer, “Motor adaptation as a greedy optimization of error and effort,” *Journal of neurophysiology*, vol. 97, no. 6, pp. 3997–4006, 2007.
- [15] A. Koenig, X. Omlin, L. Zimmerli, M. Sapa, C. Krewer, M. Bolliger, F. Müller, and R. Riener, “Psychological state estimation from physiological recordings during robot-assisted gait rehabilitation,” *Journal of Rehabilitation Research & Development*, vol. 48, no. 4, 2011.
- [16] R. Begg and J. Kamruzzaman, “A machine learning approach for automated recognition of movement patterns using basic, kinetic and kinematic gait data,” *J. Biomechanics*, vol. 38, no. 3, pp. 401–408, 2005.
- [17] J. Wu, J. Wang, and L. Liu, “Feature extraction via KPCA for classification of gait patterns,” *Human Movement Sci.*, vol. 26, no. 3, pp. 393–411, 2007.
- [18] M. Yang, H. Zheng, H. Wang, S. McClean, J. Hall, and N. Harris, “A machine learning approach to assessing gait patterns for complex regional pain syndrome,” *Medical Eng. & Physics*, vol. 34, no. 6, pp. 740–746, 2012.
- [19] P. Tahafchi, R. Molina, J. A. Roper, K. Sowalsky, C. J. Hass, A. Gunduz, M. S. Okun, and J. W. Judy, “Freezing-of-gait detection using temporal, spatial, and physiological features with a support-vector-machine classifier,” *IEEE Int. Conf. Eng. in Medicine and Biology Soc.*, no. 352, pp. 2867–2870, 2017.
- [20] W. B. Knox and P. Stone, “Interactively shaping agents via human reinforcement: The TAMER framework,” *Proc. 5th Int. Conf. Knowledge Capture*, pp. 9–16, 2009.
- [21] P. M. Pilarski, M. R. Dawson, T. Degris, F. Fahimi, J. P. Carey, and R. S. Sutton, “Online human training of a myoelectric prosthesis controller via actor-critic reinforcement learning,” *Proc. IEEE Int. Conf. Rehab. Robotics*, pp. 134–140, 2011.
- [22] S. Griffith, K. Subramanian, and J. Scholz, “Policy shaping: Integrating human feedback with reinforcement learning,” *Advances Neural Inform. Process. Syst.*, pp. 2625–2633, 2013.
- [23] P. F. Christiano, J. Leike, T. Brown, M. Martic, S. Legg, and D. Amodei, “Deep reinforcement learning from human preferences,” in *Advances Neural Inform. Process. Syst.*, 2017, pp. 4302–4310.
- [24] N. Wilde, D. Kulić, and S. L. Smith, “Learning user preferences in robot motion planning through interaction,” in *Proc. IEEE Int. Conf. Robotics and Automation*, 2018, pp. 619–626.
- [25] A. D. D. Dorsa Sadigh, S. Sastry, and S. A. Seshia, “Active preference-based learning of reward functions,” in *Robotics: Science and Systems*, 2017.
- [26] C. Basu, M. Singhal, and A. D. Dragan, “Learning from richer human guidance: Augmenting comparison-based learning with feature queries,” in *Proc. ACM/IEEE Int. Conf. Human-Robot Interaction*, 2018, pp. 132–140.
- [27] M. Menner and M. N. Zeilinger, “A user comfort model and index policy for personalizing discrete controller decisions,” in *Proc. Eur. Control Conf.*, 2018, pp. 1759–1765.
- [28] A. Y. Ng, S. J. Russell *et al.*, “Algorithms for inverse reinforcement learning,” in *Proc. 17th Int. Conf. Machine Learning*, vol. 1, 2000, p. 2.
- [29] P. Abbeel and A. Y. Ng, “Apprenticeship learning via inverse reinforcement learning,” in *Proc. 21st Int. Conf. Machine Learning*, 2004, p. 1.
- [30] B. D. Ziebart, A. L. Maas, J. A. Bagnell, and A. K. Dey, “Maximum entropy inverse reinforcement learning,” in *Proc. 23rd AAAI Conf. Artificial Intelligence*, vol. 8, 2008, pp. 1433–1438.
- [31] S. Levine, Z. Popovic, and V. Koltun, “Nonlinear inverse reinforcement learning with gaussian processes,” in *Advances Neural Inform. Process. Syst.*, 2011, pp. 19–27.
- [32] D. Hadfield-Menell, S. J. Russell, P. Abbeel, and A. Dragan, “Cooperative inverse reinforcement learning,” in *Advances Neural Inform. Process. Syst.*, 2016, pp. 3909–3917.
- [33] K. Bogert, J. F.-S. Lin, P. Doshi, and D. Kulić, “Expectation-maximization for inverse reinforcement learning with hidden data,” in *Proc. Int. Conf. Autonomous Agents & Multiagent Syst.*, 2016, pp. 1034–1042.
- [34] V. Joukov and D. Kulić, “Gaussian process based model predictive controller for imitation learning,” in *IEEE-RAS 17th Int. Conf. Humanoid Robotics*, 2017, pp. 850–855.
- [35] K. Mombaur, A. Truong, and J.-P. Laumond, “From human to humanoid locomotion: An inverse optimal control approach,” *Autonomous robots*, vol. 28, no. 3, pp. 369–383, 2010.
- [36] D. Clever, R. M. Schemschat, M. L. Felis, and K. Mombaur, “Inverse optimal control based identification of optimality criteria in whole-body human walking on level ground,” in *6th IEEE Int. Conf. Biomedical Robotics and Biomechatronics*, 2016, pp. 1192–1199.
- [37] J. F.-S. Lin, V. Bonnet, A. M. Panchea, N. Ramdani, G. Venture, and D. Kulić, “Human motion segmentation using cost weights recovered from inverse optimal control,” in *IEEE-RAS 16th Int. Conf. Humanoid Robots*, 2016, pp. 1107–1113.
- [38] P. Englert, N. A. Vien, and M. Toussaint, “Inverse KKT: Learning cost functions of manipulation tasks from demonstrations,” *Int. J. Robotics Res.*, vol. 36, no. 13–14, pp. 1474–1488, 2017.
- [39] M. Menner and M. N. Zeilinger, “Convex formulations and algebraic solutions for linear quadratic inverse optimal control problems,” in *European Control Conference*, 2018, pp. 2107–2112.
- [40] M. Menner, P. Worsnop, and M. N. Zeilinger, “Predictive modeling by infinite-horizon constrained inverse optimal control with application to a human manipulation task,” *arXiv preprint arXiv:1812.11600*, 2018.
- [41] A. L. E. N. Kleebsattel and K. Mombaur, “Inverse optimal control based enhancement of sprinting motion analysis with and without running-specific prostheses,” in *7th IEEE Int. Conf. Biomedical Robotics and Biomechatronics*, 2018, pp. 556–562.
- [42] R. S. Sutton and A. G. Barto, *Reinforcement learning: An introduction*. MIT press, 1998.
- [43] C. M. Bishop, *Pattern Recognition and Machine Learning*. Secaucus, NJ: Springer, 2006.
- [44] J. Perry, *Gait Analysis: Normal and Pathological Function*. Thorofare, NJ: SLACK Incorporated Inc., 1992.
- [45] G. James, D. Witten, T. Hastie, and R. Tibshirani, *An introduction to statistical learning*. New York: Springer, 2013, vol. 112.